Neutron diffraction study of the non-Fermi liquid compound CeNiGa2: magnetic behaviour as a function of pressure and temperature

Vincent Legrand, Winfried Kockelmann, Christopher D Frost, Robert Hauser, Dariusz Kaczorowski

Neutron diffraction study of the non-Fermi liquid compound $CeNiGa_2$: magnetic behaviour as a function of pressure and temperature

V Legrand[1], W Kockelmann[2], C D Frost[2], R Hauser[3,5] and D Kaczorowski[4]

[1] LUNAM Université, Université de Nantes—Centrale Nantes, Institut de Recherche en Génie Civil et Mécanique (UMR CNRS 6183), 37 boulevard de l'Université, BP 406, F-44602 Saint-Nazaire cedex, France
[2] Rutherford Appleton Laboratory, ISIS Facility, Chilton, Oxon, OX11 0QX, UK
[3] Institut für Experimentalphysik, Technische Universität Wien, A-1040 Wien, Austria
[4] Institute of Low Temperature and Structure Research, Polish Academy of Sciences, 50-950 Wroclaw 2, PO Box 1410, Poland

E-mail: vincent.legrand@univ-nantes.fr

Abstract
The magnetic symmetry and structure of the non-Fermi liquid heavy fermion compound $CeNiGa_2$ has been determined by neutron powder diffraction. The orthorhombic $CeNiGa_2$ compound orders antiferromagnetically below 4.4(2) K at ambient pressure with a magnetic moment magnitude of $\mu_{Ce} = 0.80(4)\ \mu_B$ for moments aligned along the c-axis. The magnetic (Shubnikov) space group is $C_{2c}m'm'm$. The nature of the magnetic order of $CeNiGa_2$ is further elucidated by neutron diffraction at elevated pressures up to 4.5 kbar, allowing for the confirmation of a critical pressure P_C of about 4.2(2) kbar above which the magnetic moment ordering is suppressed.

1. Introduction

For some years, a number of heavy fermion systems have been investigated where marked departures from the Fermi liquid predictions have been observed [1]. Such materials have been labelled non-Fermi liquids [2]. One regime where non-Fermi liquid behaviour has been observed is in the proximity of a quantum phase transition which occurs at zero temperature, driven by quantum fluctuations rather than thermal fluctuations, where the former can be driven by parameters such as pressure, magnetic field or chemical substitution. There is considerable theoretical and experimental interest in the achievement of the phase diagram associated with the development of a non-Fermi liquid state. Examples have been found in several systems, e.g. $CeNi_2Ge_2$ [3] or $CeNiGa_2$ [4–6]. Such studies have mostly relied on measurements of macroscopic properties of the materials, such as heat capacity, susceptibility measurements and resistivity as a function of hydrostatic pressure or chemical composition [7, 8]. Novel partial long-range order phases have been observed in the non-Fermi liquid phase regime of MnSi above a certain pressure P_C [9–12].

$CeNiGa_2$ is of the $NdNiGa_2$ structure type that crystallizes in space group *Cmmm* [13]. $CeNiGa_2$ is known to be an antiferromagnetic ordered Kondo lattice with a magnetic ordering temperature of about $T_N = 4$ K. While this magnetic transition has been observed using several experimental techniques based on measurements of the magnetic, thermal and transport properties [4], the magnetic symmetry and moment directions remain undetermined. In particular, this

[5] Present address: Fachhochschule Kärnten, A-9800 Spittal, Austria.

is because single crystals have not been grown and also due to the assumed small ordered magnetic moments of Ce. It has been shown that hydrostatic pressure of about 4 kbar is sufficient to drive T_N towards zero [6], i.e. close to quantum phase transition. Resistivity measurements show that the compound exhibits Fermi liquid behaviour at ambient pressure which is lost as the quantum phase transition is approached [5, 6], giving way to a $T^{3/2}$ dependence which has been observed in other systems. Like other systems, further increasing the pressure away from the quantum phase transitions leads to a recovery of the Fermi liquid behaviour again. Here, we report on the direct investigation of the microscopic antiferromagnetic structure of $CeNiGa_2$ by the method of neutron diffraction on powder samples performed at low temperatures down to 1.4 K, i.e. in the Fermi liquid regime. The aim of the study was also to examine the magnetic ordering of $CeNiGa_2$ at low temperature and when hydrostatic pressure is applied above a critical pressure P_C of about 4 kbar, i.e. where non-Fermi liquid behaviour has been postulated [6].

2. Experimental details

Powder samples of $CeNiGa_2$ were prepared by conventional solid-state reaction techniques (Czochralski pulling method). Powder diffraction data on $CeNiGa_2$ at ambient pressure and low temperature (1.4–8 K) were collected on the angle dispersive G4.1 diffractometer at the Orphée research reactor, LLB-Saclay, France. The sample was filled into a vanadium container and cooled down in a He cryostat down to 1.4 K. The neutron wavelength was 2.426 Å. Time-of-flight neutron diffraction patterns were collected at ambient and elevated hydrostatic pressures (up to 4.5 kbar) and low temperature (1.7–300 K) on the time-of-flight diffractometers ROTAX and OSIRIS at the pulsed neutron spallation source ISIS at the Rutherford Appleton Laboratory, UK. ROTAX is a medium resolution neutron diffractometer [14]; OSIRIS [15] is characterized by a high resolution of $\Delta d/d = 0.2\%$ in the d-spacing of the magnetic Bragg peaks of $CeNiGa_2$.

Pressure dependent measurements were performed using a high pressure He gas intensifier cell, made of type 7075 aluminium alloy. Pressure experiments were performed up to a hydrostatic gas pressure of 4.5 kbar. The pressure cell was inserted into a He flow 'orange' cryostat. The major experimental difficulties with such a sample environment are the background scattering from the cell material and the determination of the pressure in the solidified He medium. In a first run on ROTAX, diffraction data were collected with the $CeNiGa_2$ powder alone. Additional diffraction data were then collected on the OSIRIS diffractometer with 10 wt% of a NaCl powder mixed with the $CeNiGa_2$ powder. Pressure values were obtained by using two NaCl Bragg peaks to calculate the volume change from a reference volume (at 298 K, ambient pressure) and tabulated values given in [16].

The powder material was filled into the Al cell which was inserted into the standard orange cryostat. The neutron beam on ROTAX was collimated down to a beam cross section of 5×30 mm^2 in order to minimize the scattering from the pressure cell, i.e. about 600 mm^3 of powder material was irradiated. The beam size on OSIRIS was 20×40 mm^2. The error of the sample temperature measurement is estimated to be 0.2 K. The pressure reading error is about 0.2 kbar. Data were collected in forward scattering on ROTAX, with a detector bank at 33°, yielding a d-spacing range of 2.5–8.0 Å, not containing aluminium Bragg peaks from the sample cell. On OSIRIS, data were collected in backscattering in a d-spacing range of 1–7 Å.

Table 1. Atomic positions and lattice parameters for $CeNiGa_2$ at RT and 8 K.

	x	y	z
		RT	
Ce	0.00	0.3590(6)	0.50
Ni	0.00	0.0725(2)	0.00
Ga(1)	0.00	0.2091(3)	0.00
Ga(2)	0.00	0.00	0.50
Ga(3)	0.50	0.00	0.00
a, b, c (Å)	4.2211(4)	17.586(1)	4.1798(4)
		8 K	
Ce	0.00	0.3607(8)	0.50
Ni	0.00	0.0682(3)	0.00
Ga(1)	0.00	0.2034(4)	0.00
Ga(2)	0.00	0.00	0.50
Ga(3)	0.50	0.00	0.00
a, b, c (Å)	4.2140(6)	17.576(4)	4.1761(5)

In summary, powder diffraction data on $CeNiGa_2$ at ambient pressure were collected on the diffractometers G4.1 (1.4–8 K) and ROTAX (1.7–300 K), and at high pressure up to 4.5 kbar on the diffractometers ROTAX and OSIRIS (1.8–8 K). Rietveld profile analyses of the angle dispersive and time-of-flight data collection were performed using the FullProf [17] and GSAS [18] programs. The following nuclear scattering lengths were used: $b_{Ce} = 4.840$ fm, $b_{Ni} = 10.300$ fm and $b_{Ga} = 7.288$ fm [19]. The magnetic form factor of the Ce^{3+} ion was derived from [20].

3. Results and discussion

3.1. Nuclear and magnetic structure at ambient pressure

Structural refinements were performed at ambient temperature (RT) and 8 K. $CeNiGa_2$ is of the $NdNiGa_2$ structure type that crystallizes in the orthorhombic space group *Cmmm* [13] (figure 1). To perform the Rietveld refinements, the instrumental parameters, cell parameters, atomic positions, occupancies and atomic displacement parameters were allowed to vary. The refined lattice parameters from neutron diffraction are $a = 4.2211(4)$ Å, $b = 17.586(1)$ Å and $c = 4.1798(4)$ Å at RT. Cooling to 8 K induces a small contraction of the lattice parameters giving rise to the following lattice parameters: $a = 4.2140(6)$ Å, $b = 17.576(4)$ Å and $c = 4.1761(5)$ Å. Table 1 gives the refined atomic positions for $CeNiGa_2$ at RT and 8 K. The structural parameters listed in table 1 indicate small changes of the atomic positions.

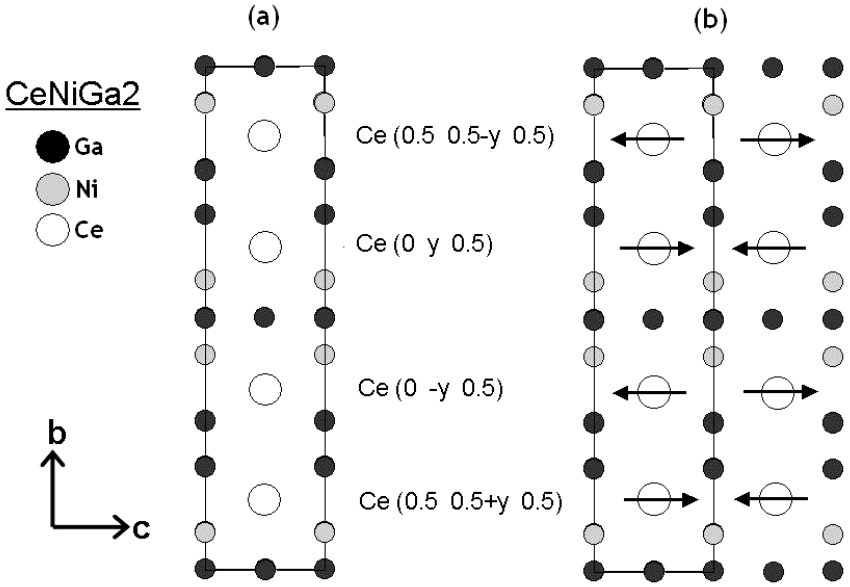

Figure 1. $CeNiGa_2$: schematic positions of the atoms in (a) the refined crystal unit cell and (b) the magnetic unit cell doubled along the *c*-crystallographic axis due to a [0, 0, 1/2] propagation vector. The arrow on the Ce atoms, aligned along the *c*-axis, symbolizes the Ce-ordered magnetic moment.

A way to observe a small magnetic component of a diffraction pattern is to separate it from the structural component by subtracting the diffraction patterns recorded well above and below the magnetic ordering temperature. The subtraction procedure of the 8 K and T ($T < T_N$) patterns should give only the magnetic diffraction pattern. Only seven magnetic peaks are sufficiently intense to be eligible for refinement at $T < T_N$. All the structural parameters are constrained to those found at 8 K, and only the orientation and the magnitude of the Ce magnetic moment are allowed to refine.

Diffraction scans with a scattering angle over the range $14° < 2\theta < 64°$ allow measurement of the most intense magnetic peaks. Figure 2 shows the results of the 2θ scan taken at various temperatures between 1.4 and 8 K. In the 8 and 4.5 K diffraction patterns, only the nuclear peaks are observed. As soon as the measuring temperature is below the magnetic ordering temperature, magnetic peaks are then observed in addition to the nuclear ones, with increasing intensity as the temperature decreases. The magnetic reflection positions are not coincident with the nuclear Bragg peak positions, which implies that the magnetic unit cell differs from the nuclear unit cell. The indexing of the magnetic lines requires doubling of the unit cell in the *c* direction; the magnetic peaks appear at $T < T_N$ at positions displaced from the nuclear peaks by $\pm(0, 0, 1/2)$. This is mostly observable in figure 3, which shows the difference intensity curve between the 1.4 K scan and the 8 K scan. The (0 2 1), at $2\theta = 23.6°$, and the (1 1 1), at $2\theta = 38.54°$, magnetic reflections have the largest intensity variations. The changes in the peak intensities of the (0 2 1) (figure 4(a)) and (1 1 1) reflections as a function of temperature confirm that these peaks are due to magnetic order, with a Néel temperature of $T_N = 4.4(2)$ K, which is in agreement with previous magnetic susceptibility and specific heat measurements [4]. The transition is continuous and no hysteresis is observed.

In the case of the $CeNiGa_2$ compound only the Ce atom carries a magnetic moment. The magnitude and direction were determined from the neutron diffraction data. For the antiferromagnetic ordered structure with a $[0, 0, 1/2]$ propagation vector only a small number of possible Ce spin arrangements need to be considered. The basic structures have spin directions along the *a*, *b*- or *c*-crystallographic axes, for which simulations of diffraction patterns were carried out, with parallel and antiparallel arrangements, using the space group $P1$, as the magnetic space group was unknown. Moreover, based on the 1.4 K measured data and on the 8 K refined parameters, simulations were performed assuming Ce atom magnetic moment values of 0.5 μ_B and 0.8 μ_B. Thus, we considered a total of 12 (3 orientations $\times$ 2 spin arrangements $\times$ 2 moment magnitudes) basic possibilities to simulate the magnetic neutron patterns. One of them is represented in figure 1 (antiparallel arrangement along the *c*-axis). These magnetic moment values were not chosen at random. An ordered moment value of 0.5 μ_B is at the limit of detection for the powder diffractometers used. Moreover, it can be noted that many Ce-based compounds adopt magnetic ground states, the properties of which are determined by the interplay of short-range Kondo interactions and long-range magnetic Ruderman–Kittel–Kasuya–Yosida (RKKY) interactions. Salient features of such systems are, e.g., large specific heat values linear in T in the ordered state and reduced zero-field magnetic moments [8]. For example, the compounds $CeInSn_2$ (0.5 μ_B; $T_N = 10$ K; [21]), $CeAl_2$ (0.89 μ_B; $T_N = 3.8$ K; [22]), $CeIn_3$ (0.48 μ_B; $T_N = 10$ K; [22]) or $CePd_2Si_2$ (0.62–0.66 μ_B; $T_N = 9.9$ K; [7]) show reduced magnetic moments relative to the value of 2.54 μ_B found in the Ce^{3+} free ion.

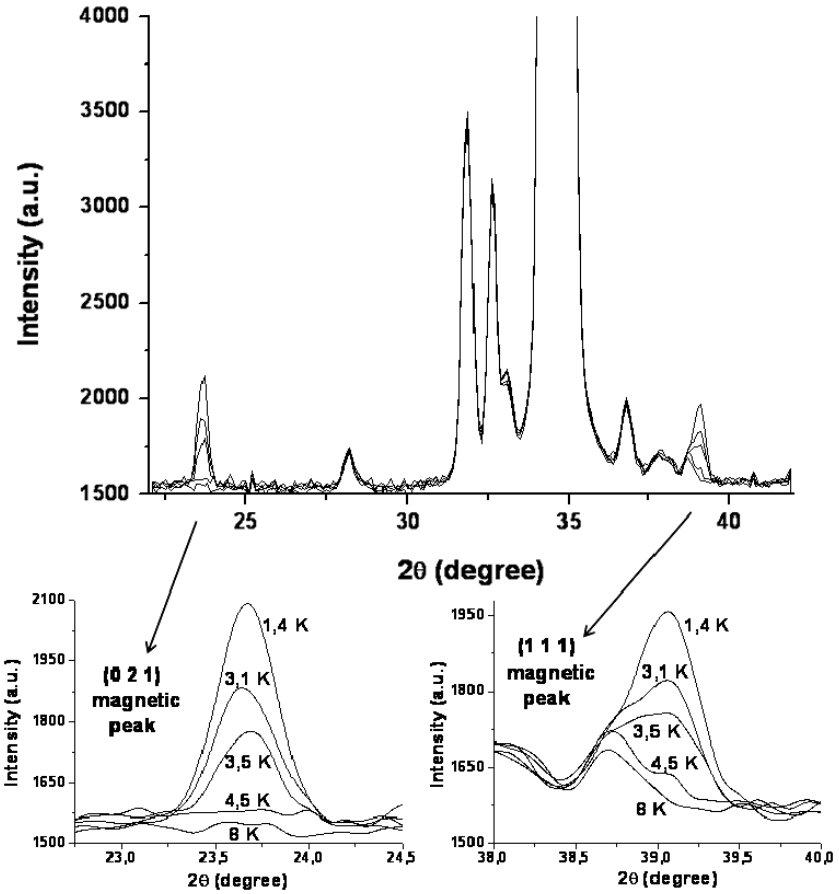

Figure 2. The diffraction patterns of $CeNiGa_2$ at various temperatures between 1.4 and 8 K. The detailed intensity variation of the (0 2 1) and (1 1 1) magnetic reflections is shown.

The comparison of the 1.4 K measured and simulated patterns obtained considering different spin directions and assuming a magnetic moment value of 0.8 μ_B clearly shows that the (0 2 1) (d-spacing = 6.05 Å, $2\theta = 23.6°$) and (1 1 1) (d-spacing = 3.68 Å, $2\theta = 38.54°$) magnetic peaks appear well defined considering magnetic moment direction along the b- or c-axes. The calculated magnetic intensities do not agree with models having magnetic moments along the a-axis of the orthorhombic unit cell. From the measured magnetic data alone it was not possible to distinguish moment directions along the b-axis and c-axis. Thus, we arbitrarily chose to refine the magnetic parameters at $T = 1.4$ K in the $P1$ space group with a fixed magnetic moment component along the c-axis as the magnetic unit cell is doubled along this axis. The refined magnetic moment magnitude is 0.80(4) μ_B, which is smaller than the theoretical value (2.54 μ_B) expected for the Ce^{3+} ion. The reduction of the moment magnitude in $CeNiGa_2$ is reminiscent of the values in other reduced moment compounds [7, 21, 22]. Finally, we also refined the magnetic parameters of $CeNiGa_2$ at 2.6, 3.1, 3.5, 4.0 and 4.5 K to determine the dependence of the magnetic moment magnitude as a function of temperature (figure 4(b)). The temperature variation of the magnetic moment can be explained well with a phenomenological power law behaviour $\mu_B(T) \propto (1 - \frac{T}{T_N})^\beta$, with $T_N = 4.5(1)$ K corroborating the

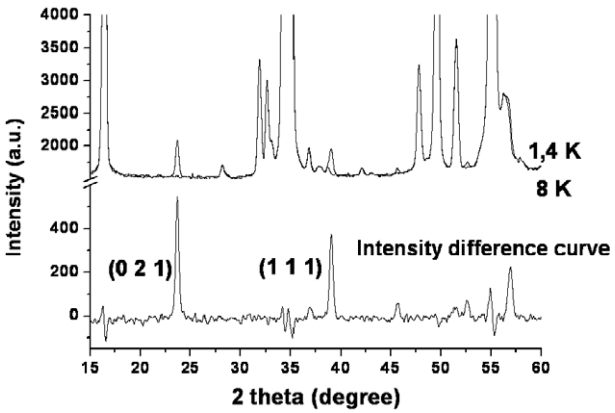

Figure 3. The diffraction patterns of $CeNiGa_2$ at 1.4 K and 8 K are plotted with the corresponding difference curve.

Néel temperature of $T_N = 4.4(2)$ K obtained previously. The exponent β is obtained to be 0.30(2).

This analysis is independent of any hypothesis about the symmetry of the magnetic structure of the present compound, other than that the antiferromagnetic moment lies along the c-crystallographic axis. To investigate the magnetic symmetry of $CeNiGa_2$, the Shubnikov groups corresponding to the nuclear space group *Cmmm* were analysed. The *Cmmm*

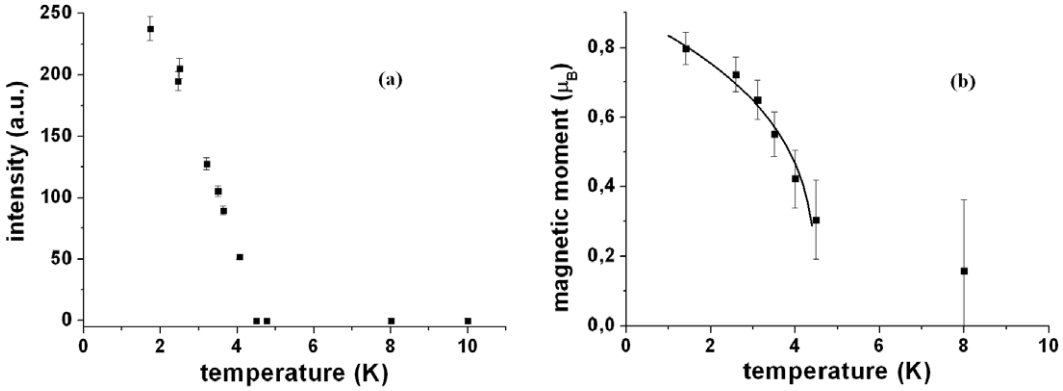

Figure 4. (a) Intensity variation of the (0 2 1) magnetic peak as a function of temperature at ambient pressure. (b) Temperature dependence of the magnetic moment magnitude at ambient pressure; the line represents the phenomenological power law behaviour $\mu_B(T) \propto (1 - \frac{T}{T_N})^\beta$ (see text for details).

symmetry allows 29 possible magnetic space groups [23]. From our structural refinements it is known that the C-centre lattice is preserved, that the Ce atoms are on a Wyckoff 4j position in the *Cmmm* nuclear space group and that the magnetic cell is linked to a $[0, 0, 1/2]$ propagation vector along the *c*-axis. Among the Shubnikov groups, only the magnetic space group $C_{2c}m'm'm$ is feasible, and in agreement with the observed magnetic Bragg peaks.

To determine the value and the direction of the magnetic moment with certainty, one would need to perform polarized neutron measurements on a single crystal. For example, the D3 diffractometer at the Institut Laue Langevin (Grenoble, France) coupled with the Cryopad sample environment (for zero-field neutron polarimetry measurement) would be well suited to study of the antiferromagnetic structure of $CeNiGa_2$ and the magnetic moment orientation. Moreover, polarized neutrons coupled with a cryomagnet environment could also be envisaged to investigate the magnetization density induced by an external field, which would allow the description of the Ce–Ce magnetic interactions and the eventual existence of a slight Ce–Ni interaction, as shown in other CeNi-containing compounds [24].

3.2. Magnetic ordering at high pressures

The magnetic behaviour of $CeNiGa_2$ was investigated at high pressure up to 4.5 kbar in the temperature range 1.8–5 K. The instrument setup was optimized to analyse the intensity variation of the (0 2 1) and (1 1 1) magnetic reflections. Neutron diffraction patterns were recorded in steps of about 0.3 K for all applied pressures to fully observe the antiferromagnetic domain of the (P, T) diagram. It is important to notice that the pressure measurements reported here were the first ones performed on $CeNiGa_2$.

Magnetic Bragg peaks are observed at elevated pressures at the same *d*-spacing values as for the ambient pressure measurements. Moreover, the ratios of the magnetic Bragg peaks do not change with pressure. This indicates that the symmetry and type of magnetic order does not change with applied hydrostatic pressure up to the critical pressure P_C at

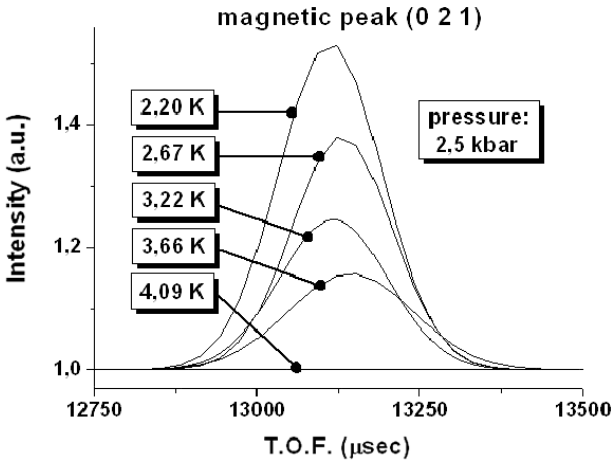

Figure 5. Intensity of the (0 2 1) magnetic peak at 2.5 kbar as a function of temperature.

which the magnetic moment falls down to zero. We have used this observation to simplify the magnetic structure model used in the data fitting below.

Figure 5 shows the fitted intensity variation of the (0 2 1) magnetic peak at $P = 2.5$ kbar for five different temperatures. As the temperature increases we observe the decrease of the peak intensity as expected and the Néel temperature is determined as $T_N = 3.7(4)$ K at 2.5 kbar. Even if the background intensity is higher due to the presence of the pressure cell in addition to the cryostat, magnetic peaks always show well defined shapes and are sufficiently intense to allow the analysis of the magnetic moment dependence as a function of pressure and temperature, as shown in figure 6. The determination of the magnetic moment is based on the Rietveld refinement of the neutron patterns, but because only a few magnetic peaks are present and they appear in the pattern with low intensity, the structural parameters refined at 8 K were considered as a reference for the low temperature structures and only the scale factor and the magnetic moment values were refined for $T < T_N$. The application of pressure causes a reduction of the ordering temperature. For example, we observe for measurements at the lower temperature

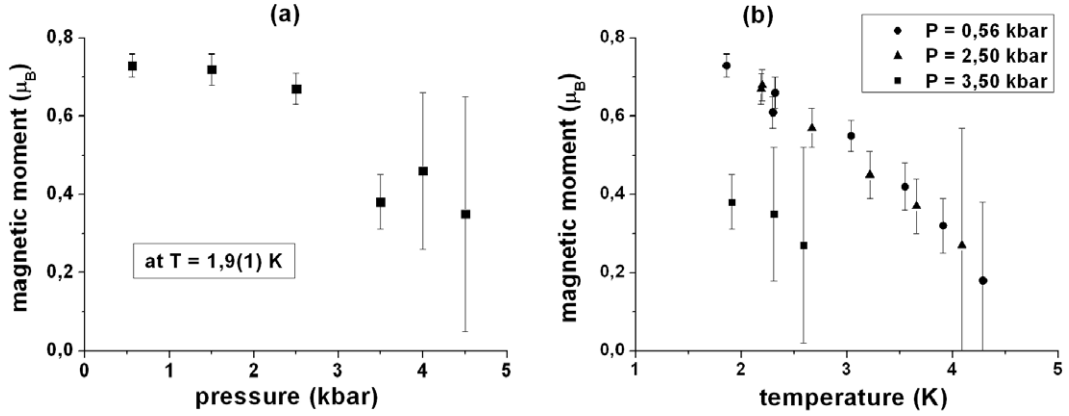

Figure 6. (a) Pressure dependence at $T = 1.9(1)$ K and (b) temperature dependence at various pressures of the magnetic moment magnitude for the ROTAX data.

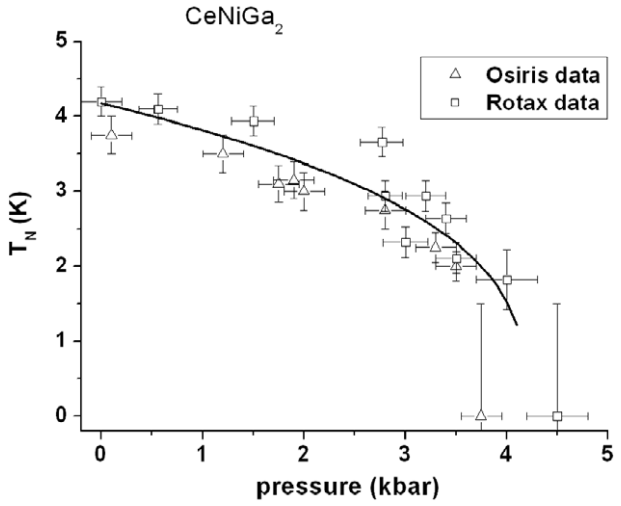

Figure 7. Pressure dependence of the Néel temperature. The line represents the typical phenomenological power law behaviour $T_N \propto (P_C - P)^x$ (see text for details). Note: the minimum experimental temperature was 1.7 K, hence the large error bars on the data points for $T_N = 0$ K.

1.9(1) K (figure 6(a)) that for pressures below about 3 kbar, the magnetic moment stays approximately stable with an average value of 0.71(3) μ_B. Above 3 kbar, the value of the magnetic moment decreases and is about 0.40(6) μ_B. The values of T_N for each applied pressure were determined and are represented in figure 7. The application of pressure induces a decrease of the antiferromagnetic ordering temperature. T_N is rapidly shifted towards zero following a phenomenological power law behaviour $T_N \propto (P_C - P)^x$, where $x = 0.33(2)$ ensures the best fit. Then, the critical pressure P_C, i.e. the pressure at which T_N vanishes, is obtained to be 4.2(2) kbar.

This value of P_C, found by the neutron diffraction OSIRIS and ROTAX experimental data, is in agreement with the one calculated by resistivity measurements (P_C around 4 kbar) [6]. In this study, the pressure was limited to a maximum value of 4.5 kbar due to the specificity of the pressure aluminium cell used. The measurements on OSIRIS indicate that the hydrostatic pressures on the $CeNiGa_2$ sample were slightly lower.

4. Conclusions

This neutron diffraction study of $CeNiGa_2$ highlighted that the value of the Ce^{3+} magnetic moment in the ordered antiferromagnetic state is 0.80(4) μ_B at 1.4 K under ambient pressure. Thus, the magnetic moment is reduced to about 30% in comparison to the free ion, indicating partial Kondo screening of the moment. Moreover, this reduced value of the magnetic moment could also be due to the crystal field effect. The Néel temperature $T_N = 4.4(2)$ K was also confirmed. The temperature dependence of the magnetic moment magnitude was investigated and described using a phenomenological law $\mu_B(T) \propto (1 - \frac{T}{T_N})^\beta$. This analysis was based on data refined considering a magnetic structure with a [0, 0, 1/2] propagation vector and a magnetic moment aligned along the c-crystallographic axis. The magnetic (Shubnikov) space group of $CeNiGa_2$ is $C_{2c}m'm'm$. Further work will use single crystals to perform polarized neutron diffraction measurements to confirm the orientation and direction of the Ce^{3+} magnetic moment and to investigate the magnetization density in $CeNiGa_2$. In particular, the latter measurement could give supplementary details about the observed reduced value of the magnetic moment, as few materials exhibit modulated moments with Ce-ordered moments varying from site to site and driving to zero at certain sites [25]. The magnetic behaviour of the sample was described under hydrostatic pressure up to 4.5 kbar in the temperature range 1.7–5 K. With pressure the balance between the RKKY interactions and the Kondo interactions can be tuned and the magnetism is suppressed. We have shown that the Néel temperature follows a $T_N \propto (P_C - P)^x$ law. The application of pressure induces a decrease of the antiferromagnetic ordering temperature at a critical pressure of $P_C = 4.2(2)$ kbar. Finally, even under applied pressure, magnetic and nuclear peaks were measured always at the same position in 2θ indicating no change in the magnetic structure (symmetry or moment direction) or in the nuclear structure.

Acknowledgments

The authors express their gratitude to the LLB reactor (France) and to the ISIS spallation source (UK) for provision of the neutron beamtime and making the instruments available.

References

[1] Mathur N D, Grosche F M, Julian S R, Walker I R, Freye D M, Haselwimmer R K W and Lonzarich G G 1998 *Nature* **394** 39
[2] Schofield A J 1999 *Contemp. Phys.* **40** 95
[3] Sato H, Aoki Y, Urakawa J, Matsuda T D, Sugawara H, Fukuhara T and Maezawa K 1998 *J. Magn. Magn. Mater.* **177–181** 409
[4] Aoki Y, Terayama K and Sato H 1995 *J. Phys. Soc. Japan* **64** 3986
[5] Hauser R, Galli M, Bauer E, Kottar A, Hilscher G and Kaczorowski D 1998 *J. Magn. Magn. Mater.* **177–181** 292
[6] Hauser R, Bauer E, Hilscher G, Michor H and Kaczorowski D 1997 *Physica* B **237/238** 205
[7] Besnus M J, Braghta A, Hamdaoui N and Meyer A 1992 *J. Magn. Magn. Mater.* **104–107** 1385
[8] Löhneysen H V 1996 *J. Phys.: Condens. Matter* **8** 9689
[9] Pfleiderer C, Julian S R and Lonzarich G G 2001 *Nature* **414** 427
[10] Pfleiderer C, Reznik D, Pintschovius L, Löhneysen H V, Garst M and Rosch A 2004 *Nature* **427** 227
[11] Pfleiderer C, Reznik D, Pintschovius L and Haug J 2007 *Phys. Rev. Lett.* **99** 156406
[12] Pfleiderer C, Neubauer A, Mühlbauer S, Jonietz F, Janoschek M, Legl S, Münzer W, Franz C, Niklowitz P G, Keller T, Georgii R, Böni P, Binz B, Rosch A, Rößler U K and Bogbanov A N 2009 *J. Phys.: Condens. Matter* **21** 164215
[13] Romaka V A, Grin Y N, Yarmolyuk Y P, Skolozdra R V and Yartys A A 1983 *Ukr. Fiz. Zh.* **28** 227
[14] Kockelmann W, Weißer M, Heinen H, Kirfel A and Schäfer W 2000 *Mater. Sci. Forum* **321–324** 332
[15] Telling M T F and Andersen K H 2005 *Phys. Chem. Chem. Phys.* **7** 1255
[16] Skelton E F, Webb A W, Qadri S B, Wolf S A, Lacoe R C, Feldman J L, Elam W T, Carpenter E R Jr and Huang C Y 1984 *Rev. Sci. Instrum.* **55** 849
[17] Rodriguez-Carvajal J 1993 *Physica* B **192** 55
[18] Larson A C and Von Dreele R B 1994 General structure analysis system (GSAS) *Los Alamos National Laboratory Report* LAUR 86-748
[19] Sears V F 1992 *International Tables of Crystallography* vol C, ed A J C Wilson (Dordrecht: Kluwer) p 383
[20] Brown P J 1992 *International Tables of Crystallography* vol C, ed A J C Wilson (Dordrecht: Kluwer) p 391
[21] Benoit A, Boucherle J X, Flouquet J, Sakurai J and Schweizer J 1985 *J. Magn. Magn. Mater.* **47/48** 149
[22] Boucherle J X, Flouquet J, Lassailly Y, Palleau J and Schweizer J 1983 *J. Magn. Magn. Mater.* **31–34** 409
[23] Shubnikov A V *et al* 1964 *Colored Symmetry* (Oxford: Pergamon)
[24] Hiess A, Zobkalo I, Bonnet M, Schweizer J, La E, Tasset F, Isikawa Y and Lander G H 1997 *Physica* B **230–232** 687
[25] Lawrence J 1982 *J. Appl. Phys.* **53** 2117